



Cite this: *Chem. Sci.*, 2020, **11**, 5404

All publication charges for this article have been paid for by the Royal Society of Chemistry

Received 5th April 2020
Accepted 29th April 2020

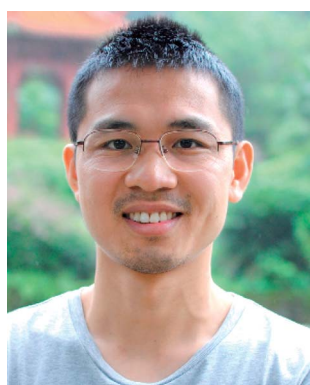
DOI: 10.1039/d0sc01936d
rsc.li/chemical-science

Introduction

Coherent light sources in the ultraviolet (UV) (<400 nm) region producing lasers with better beam quality, higher energy, and finer processing accuracy play a unique and crucial role in many newly developed scientific instruments that have opened up unprecedented opportunities for the exploration of novel phenomena in chemical science.¹ There is an endless competition on making higher energy wavelengths accessible as we go

^aCollege of Chemistry, Sichuan University, Chengdu 610064, P. R. China. E-mail: zough@scu.edu.cn

^bDepartment of Chemistry, Sogang University, Seoul 04107, Republic of Korea. E-mail: knok@sogang.ac.kr



Professor Guohong Zou earned his BS degree from Central South University in 2008, and got his PhD degree in 2013 from Fujian Institute of Research on the Structure of Matter, Chinese Academy of Sciences, China, under the direction of Professor Ning Ye on discovering new nonlinear optical materials. He performed postdoctoral research in the group of Prof. Kang Min Ok at Chung-Ang University,

Korea, on UV nonlinear optical crystals. Since joining the faculty of Sichuan University, China in 2017, he has performed research on discovering novel inorganic optical materials.

down the Moore's law road. Thus, it is a huge challenge exploring new superior performing UV nonlinear optical (NLO) materials, the most important components for solid state UV lasers. Tremendous efforts by a number of scientists over the past few decades to discover excellent NLO materials *via* elucidating the structure–property relationship resulted in several successful classical and semiclassical theoretical models.² Among them, the anionic group theory³ proposed by Chen has guided the exploration of borate UV NLO materials. A series of classical borate crystals such as β -Ba₂B₄ (BBO),⁴ LiB₃O₅ (LBO),⁵ KBe₂BO₃F₂ (KBBF),⁶ and SrBe₂BO₇ (SBBO)⁷ have been successfully discovered. Subsequently, the system was further expanded to carbonates,⁸ nitrates,⁹ phosphates,¹⁰ and sulfates.¹¹



Professor Kang Min Ok attended Sogang University, Korea, earning his BS and MS degrees in Chemistry, followed by a PhD from the University of Houston, USA, working for Professor P. Shiv Halasyamani on discovering novel second-harmonic generating solid state materials. He performed postdoctoral research in the group of Professor Dermot O'Hare at the University of Oxford, UK, on the kinetics of solid state reactions. Professor Ok worked as a distinguished scholar at Chung-Ang University (CAU), Korea. Currently, he is a Professor at Sogang University. His research includes discovering novel functional solid state materials with an asymmetric coordination environment.



A high performance UV NLO material should meet comprehensive requirements, which include crystallographic non-centrosymmetry (NCS), wide transparency, large second-order NLO coefficient ($d_{ij} > 0.39 \text{ pm V}^{-1}$), appropriate birefringence ($\Delta n \sim 0.07\text{--}0.10$ at 1064 nm), good physicochemical stability, and “easy” growth of large high-quality single crystals. The rational combination of different asymmetric polar units including anionic groups with a π -conjugate system, d^0 transition metal cations, stereochemically active lone pair (SCALP) units, and polarizable d^{10} metal cations is a general strategy that is beneficial for producing NCS NLO materials.¹² Although combining the asymmetric units during the synthesis steps significantly improved the possibility of macroscopic NCS, the major reaction products still turned out to be centrosymmetric (CS), attributable to the preference of antiparallel alignment of the asymmetric units. Since the inefficient synthetic approaches impeded the development of UV laser technology, other effective strategies toward excellent UV NLO materials are urgently required. An emerging highly effective method to discover high-performance UV NLO materials is chemical substitution-oriented design,¹³ in which one or more fundamental building units (FBUs), cations, and/or anions in a prototype phase are replaced to produce better properties. In general, to discover new UV NLO materials *via* the chemical substitution method, the following procedures are followed: (1) choice of model phases with adjustable backbones; (2) design of novel materials through chemical substitution; (3) uncovering new UV NLO compounds through the appropriate synthesis, structure determination, and NLO property measurement; (4) growing high quality large single crystals.¹⁴ In this minireview, several recently reported UV NLO materials discovered by chemical substitution-oriented design including single-site substitution, dual-site substitution, and multisite substitution are presented. Closer structural examinations for substitution of suitable functional building blocks will successfully guide the discovery of new UV NLO materials.

Single-site substitution

Single-site substitution is a general and facile strategy during the synthesis, in which one cation or anion in the parent structure is replaced by another ion in the same group of the periodic table to obtain better UV NLO properties. In general, the cations include alkali and alkaline-earth metal cations, while the anions include halide ions. Once one of the ions is substituted, the stoichiometrically similar materials often exhibit different performances due to the ion size difference.

Two novel alkali metal carbonatoperoxovanadates, $\text{A}_3\text{VO}(\text{O}_2)_2\text{CO}_3$ ($\text{A} = \text{Rb}$ and Cs),¹⁵ have been developed *via* single-site substitution after the discovery of $\text{K}_3\text{VO}(\text{O}_2)_2\text{CO}_3$ with the localized $(\text{O}_2)^{2-}$ π -orbital NLO-active unit.¹⁶ The three stoichiometrically equivalent materials share a common molecular structure, $\text{VO}(\text{O}_2)_2\text{CO}_3$ polyhedra. The backbones of $\text{A}_3\text{VO}(\text{O}_2)_2\text{CO}_3$ ($\text{A} = \text{K}$, Rb , and Cs) reveal better thermal stability as the radius of the alkali metal cations increases (Table 1). As seen in Fig. 1, since the size of K^+ in $\text{K}_3\text{VO}(\text{O}_2)_2\text{CO}_3$ is smaller, substantial interactions between K^+ cations and oxide ligands

Table 1 Thermal and optical characteristics of $\text{A}_3\text{VO}(\text{O}_2)_2\text{CO}_3$ ($\text{A} = \text{K}$, Rb , and Cs)

Compound	Dec. T (°C)	E_g (eV)	SHG ($\times \text{KDP}$)
$\text{K}_3\text{VO}(\text{O}_2)_2\text{CO}_3$	230	2.57	20
$\text{Rb}_3\text{VO}(\text{O}_2)_2\text{CO}_3$	250	2.68	21
$\text{Cs}_3\text{VO}(\text{O}_2)_2\text{CO}_3$	300	2.81	23

result in peroxy ligands with shorter O–O distances (1.456 Å) and more strained $\text{VO}_3(\text{O}_2)_2$ pentagonal bipyramids (pbps). However, the large Cs^+ cations in $\text{Cs}_3\text{VO}(\text{O}_2)_2\text{CO}_3$ with a larger coordination environment reveal peroxy ligands with longer O–O distances (1.503 Å) and less strained, more stable $\text{VO}_3(\text{O}_2)_2$ pbps. Therefore, the thermal stability of $\text{A}_3\text{VO}(\text{O}_2)_2\text{CO}_3$ ($\text{A} = \text{K}$, Rb , and Cs) increases in the order $\text{K} < \text{Rb} < \text{Cs}$ owing to the structural stability of the corresponding pbps. In addition, while $\text{K}_3\text{VO}(\text{O}_2)_2\text{CO}_3$ with the highly distorted $\text{VO}(\text{O}_2)_2\text{CO}_3$ pbps exhibits a smaller band gap, those with less strained pbps reveal larger optical gaps. Moreover, the SHG responses of $\text{A}_3\text{VO}(\text{O}_2)_2\text{CO}_3$ increase as the alkali metal cation size increases, which should be mainly attributable to the increased polarizability of larger cations along with their stronger interatomic interactions with adjacent O atoms.

The replaceable cations in single-site substitution may be bivalent cations in the emerging UV NLO metal fluoride carbonates KMCO_3F ($\text{M} = \text{Mg}$, Ca , Sr , Zn , and Cd).¹⁷ Also, the replaceable cations could be trivalent cations in $\text{Cd}_4\text{REO}(\text{BO}_3)_3$ ($\text{RE} = \text{Y}$, La , Gd , Yb , and Lu).¹⁸ Here, the SHG efficiencies increase as the polarizability of cations increases. The replaceable ions in single-site substitution could also be anions, especially halogen anions. $\text{Pb}_2\text{BO}_3\text{Cl}$ with a *trans*-KBBF structure has been proved to be a promising UV NLO crystal.¹⁹ The SHG coefficient gradually increases as the Cl^- anion is replaced by larger and more polarizable Br^- and I^- in $\text{Pb}_2\text{BO}_3\text{X}$ ($\text{X} = \text{Br}$ and I).²⁰

Dual-site substitution

As the name implies, dual-site substitution is a simultaneous replacement of two cations, anions, complex anions, or

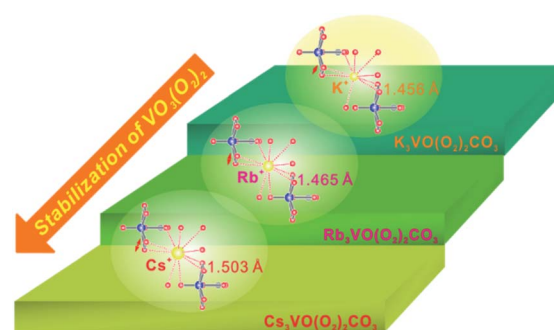
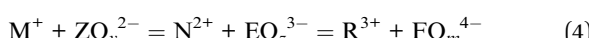
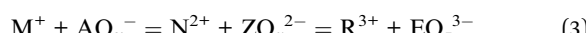
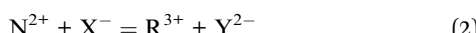
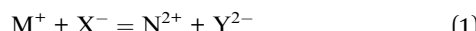


Fig. 1 Influence of the size of alkali metal cations on the stability of $\text{VO}_3(\text{O}_2)_2$ polyhedra in $\text{A}_3\text{VO}(\text{O}_2)_2\text{CO}_3$ ($\text{A} = \text{K}$, Rb , and Cs). The shorter O–O distances in peroxy ligands owing to the smaller coordination environment of K^+ result in more strained $\text{VO}_3(\text{O}_2)_2$ pbps, while the longer O–O distances in peroxy ligands due to the large Cs^+ result in less strained stable $\text{VO}_3(\text{O}_2)_2$ pbps.



fundamental building units. Although the substitution has to keep the sum of the oxidation states constant, each component is not necessarily equivalent during the replacement procedure. Dual-site substitution is an aliovalent substitution that is utilized commonly to design new materials with better performance. In order to keep the framework structure of a prototype phase, the interchangeable cations or anions should present similar sizes and structures. Proposed mechanisms for the dual-site substitution to design new UV NLO materials may include the following:



The evolution of the $KBe_2BO_3F_2$ (KBBF)⁶ family provides a perfect example of dual-site substitution (Fig. 2). It is well known that KBBF is an important deep-UV NLO material due to a large NLO coefficient, a short UV absorption cutoff edge,

and appropriate birefringence. However, its strong layered habit limits its practical application. In order to overcome the problem of layered habit during the crystal growth process and maintain all of the KBBF's excellent optical properties, $Sr_2Be_2B_2O_7$ (SBBO)⁷ was designed *via* dual-site substitution of $Sr^{2+} + O^{2-} = K^+ + F^-$. As expected, SBBO presents a perfect plane infinite $[Be_3B_3O_6]_\infty$ network which provides a large NLO coefficient and appropriate birefringence. Furthermore, the strong Be-O bonds between $[Be_3B_3O_6]$ layers are beneficial to solve the problem of layered habit in crystal growth. However, high quality large single crystals of SBBO have not been grown due to the structural polymorphism problem. Therefore, in order to stabilize the crystal structure, the proposed substitution of $F^- + Na^+ = O^{2-} + Sr^{2+}$ was applied to discover $NaCaBe_2B_2O_6F$.²¹ As we know, the constituent Be in KBBF, SBBO, and $NaCaBe_2B_2O_6F$ is highly toxic. Thus, Be-free UV NLO materials have been produced through the replacement of Be with Mg, Zn, or Al. From KBBF, KZn_2BO_3X ($X = Cl$ or Br) have been obtained by the cosubstitution of $Cl/Br^- + Zn^{2+} = F^- + Be^{2+}$. In addition, the substitution of Be with Al can also be a method to design new Be-free KBBF family materials. $K_2Al_2B_2O_7$ (ref. 22) and $BaAlBO_3F_2$ (ref. 23) have been derived from KBBF through

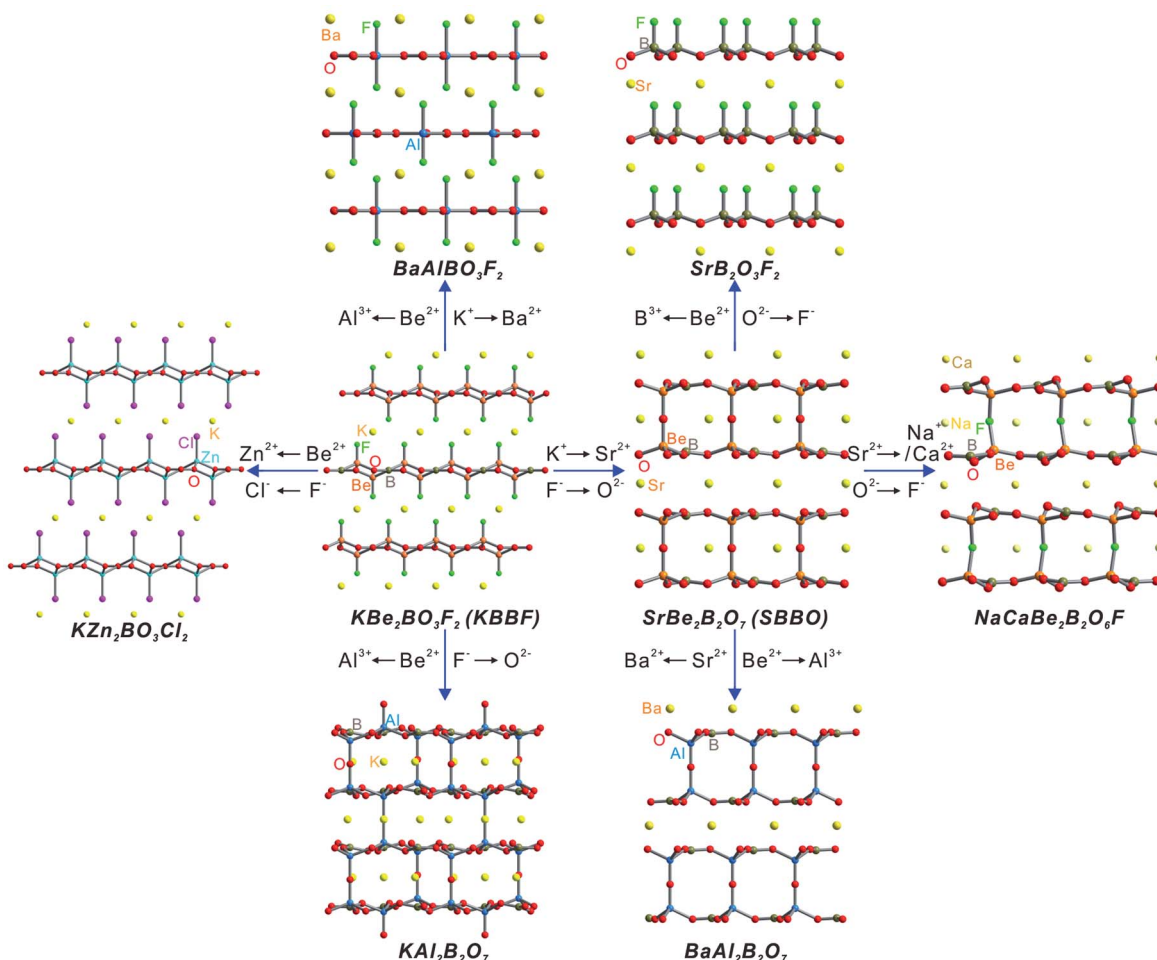


Fig. 2 Structural evolution of several KBBF-type UV NLO materials developed *via* dual-site substitutions.



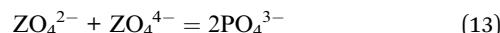
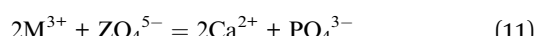
the dual-site substitution of $O^{2-} + Al^{3+} = F^- + Be^{2+}$ and $Ba^{2+} + Al^{3+} = K^+ + 2Be^{2+}$, respectively. Simultaneously, $BaAl_2B_2O_7$ (ref. 24) has been designed from SBBO by substituting $Ba^{2+} + 2Al^{3+} = 2Sr^{2+} + 2Be^{2+}$. Recently, Pan's group predicted a promising Be-free UV NLO fluorooxoborate, $Sr_2B_3O_3F_2$ (ref. 25), derived from SBBO by the substitution of $4F^- + 2B^{3+} = O^{2-} + 2Be^{2+}$. Hence, dual-site substitution is a green and effective strategy to design Be-free deep-UV NLO materials with high performance compared to the traditional trial-and-error method.

In addition to the KBBF family, dual-site substitution can also have an effect on improving the NLO properties of other systems. For example, $Pb_2TiVOF(SeO_3)_2Cl$ ²⁶ exhibited a much larger SHG coefficient than its prototype compound $Pb_2NbVO_2(SeO_3)_2Cl$ ²⁶ through the cosubstitution of $Ti^{4+} + F^- = Nb^{5+} + O^{2-}$. Also, the first bismuth selenite fluoride, $BiFSeO_3$,²⁷ reported by Mao's group revealed an enlarged SHG response, in which the novel material was designed from the parent compound iodate, $BiOIO_3$ (ref. 28), by the cosubstitution of $F^- + Se^{2-} = O^{2-} + I^-$.

Multisite substitution

Multisite substitution, as the name suggests, is the replacement of three or more cations, anions, complex anions, fundamental building units, or vacancies in prototype compounds. By far, most of the substitutions applied to design new UV NLO materials involved only two or less atomic sites with one charge difference for cations or anions, which substantially limited the diversity of structural change. If multisite substitution could be realized, the family of UV NLO materials can be greatly expanded. Firstly, we should select an appropriate prototype phase containing three or more substitutable atomic sites, in which the framework should be remarkably tolerant to structural distortion and chemical substitution. As we know, a large portion of our modern scientific database consists of a variety of minerals. Especially, a number of minerals such as apatite and perovskite presenting adaptable framework structures have significantly influenced the discovery of many novel inorganic materials with tunable physical properties in the laboratory.

For the exploration of UV NLO materials, hydroxyapatite, $Ca_5(PO_4)_3(OH)$,²⁹ is an ideal prototype structure with four substitutable atomic sites, *i.e.*, two different Ca^{2+} sites, one PO_4^{3-} site, and one OH^- site. Proposed substitution mechanisms in $Ca_5(PO_4)_3(OH)$ include the following:



According to the above mechanisms, a series of excellent UV NLO borates, $Ca_4REO(BO_3)_3$ (RE = rare earth metals),³⁰ were designed and synthesized *via* the multisite substitution of $RE^{3+} + O^{2-} + BO_3^{3-} = Ca^{2+} + OH^- + PO_4^{3-}$. Then, in order to enhance the SHG coefficient, the introduction of a d^{10} cation, Cd^{2+} , with polar displacement properties to replace Ca^{2+} , and Bi^{3+} with the stereochemically active lone pair to replace RE^{3+} produced an excellent NLO material, $Cd_4BiO(BO_3)_3$.³¹ In fact, $Cd_4BiO(BO_3)_3$ exhibited the largest NLO coefficient among borates when it was discovered owing to the three NCS chromophores. Ye's group has extended the apatite-type UV NLO materials to carbonates. The multisite substitutions of hydroxyapatite successfully produced $Na_8Lu_2(CO_3)_6F_2$ (ref. 32) and $Na_3Ca_2(CO_3)_3F$ ³³ revealing large SHG responses and appropriate birefringence.

Recently, $KTiOPO_4$ (KTP)³⁴ was selected as an ideal candidate for multisite substitution to explore new UV NLO materials. KTP is a classical commercial NLO material presenting large NLO coefficients, high thermal stability, and wide acceptance angles. However, the narrow energy bandgap (3.52 eV) hinders its practical application in the UV region. Energy band engineering has been proved to be an effective strategy to enlarge the bandgap in some materials systems. In KTP, a detailed strategy involving substituting an early transition metal, Ti^{4+} , with a main group metal to eliminate the d-p electronic transition, and substituting partial O^{2-} with F^- would induce the enlargement of the bandgap. Based on the strategy, our group developed a series of sulfates, $ASbX_2SO_4$ (A = NH_4 , Rb , or Cs ; X = F or Cl),³⁵ with a sharply enlarged bandgap (>4.7 eV) by introducing the main group Sb^{3+} cations with stereochemically active lone pairs (Fig. 3). The multisite substitution in $CsSbF_2SO_4$ is in accordance with the following scheme:

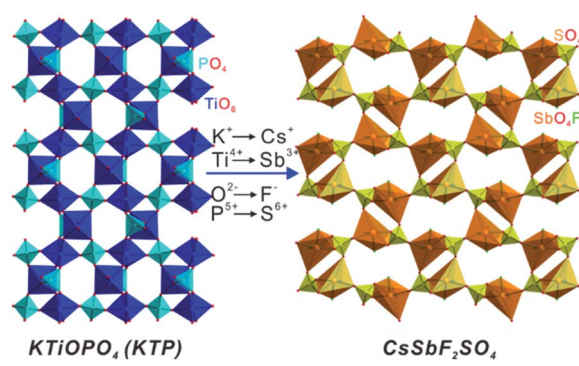
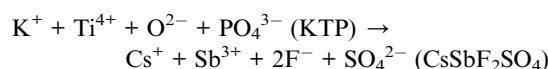


Fig. 3 Polyhedral representations showing a structural comparison between $KTiOPO_4$ and $CsSbF_2SO_4$ synthesized by multisite substitution.



From the viewpoint of structural evolution, $\text{CsSbF}_2\text{SO}_4$ can be regarded as a derivative of KTP. The 1-D $[\text{SbF}_2\text{O}_2\text{SO}_4]^{5-}$ chains produced by the interconnection of $[\text{SbF}_2\text{O}_4]^{7-}$ distorted octahedra and $[\text{SO}_4]^{2-}$ anions in $\text{CsSbF}_2\text{SO}_4$ are similar to those of $[\text{TiO}_4\text{PO}_4]^{5-}$ chains composed of $[\text{TiO}_6]^{8-}$ and $[\text{PO}_4]^{3-}$ anions in KTP. The main difference between the two structures occurs due to the introduction of fluorine atoms into the terminal sites of $[\text{SbO}_4\text{F}_2]^{7-}$ octahedra in $\text{CsSbF}_2\text{SO}_4$. While 3- and 6-membered rings (MRS) composed of bridging oxygen atoms in $[\text{TiO}_6]^{8-}$ octahedra and $[\text{PO}_4]^{3-}$ tetrahedra are observed in KTP, 4- and 8-MRS are formed in $\text{CsSbF}_2\text{SO}_4$ containing terminal fluorides (Fig. 3). Thus, KTP-type compounds have been extended to sulfate systems as novel UV NLO materials. Subsequently, RbSnFSO_4 (ref. 36) and $\text{A}_2\text{Bi}_2(\text{SO}_4)_2\text{Cl}_4$ ($\text{A} = \text{NH}_4$, K , or Rb)³⁷ with large bandgaps were successfully synthesized *via* the replacement of Ti^{4+} with Sn^{2+} and Bi^{3+} cations, respectively. Hence, the successful substitution of sulfates for phosphates may open a door to efficiently explore excellent sulfate NLO materials for UV application. Also, multisite substitution can have an effect on improving the bandgap of other systems. For example, α - and β - $\text{Ba}_2[\text{GaF}_4(\text{IO}_3)_2](\text{IO}_3)$ derived from α - and β - $\text{Ba}_2[\text{VO}_2\text{F}_2(\text{IO}_3)_2](\text{IO}_3)$ *via* multisite substitution involving one cationic and two anionic sites exhibit sharply enlarged bandgaps.³⁸

Conclusions and outlook

Chemical substitution-oriented design is a very effective strategy to explore high-performance UV NLO materials compared to the time-consuming conventional trial-and-error method. The method involves single-site, dual-site, and multi-site substitutions. The prototype phases from naturally occurring minerals or synthetic materials should present remarkable tolerance toward structural distortion and chemical substitution in order to accommodate a large number of elements or structural units. Examples of chemical substitution-oriented design to explore novel UV NLO materials include $\text{K}_3\text{VO}(\text{O}_2)_2\text{CO}_3$, KBBF , $\text{Ca}_5(\text{PO}_4)_3(\text{OH})$, and KTP-type phases. The chemical substitution approach can be easily applied to tune and extend the desired properties of solid state materials. Chemical substitution-oriented design is an emerging strategy for the exploration of novel UV NLO materials. Although a number of novel materials have been successfully discovered by virtue of the method, it should be emphasized that elucidating the intrinsic substitution mechanism of the thermodynamically stable crystalline phases, understanding the detailed crystal structures and compositions, and explaining the origin of experimentally observed physical properties on the basis of a firm theoretical background are indispensable.

Conflicts of interest

There are no conflicts to declare.

Acknowledgements

This research was supported by the National Research Foundation of Korea (NRF) funded by the Ministry of Science and ICT

(grant no. 2018R1A5A1025208 and 2019R1A2C3005530). This work was also supported by the National Natural Science Foundation of China (no. 21875146) and the Fundamental Research Funds for the Central Universities (no. YJ201921).

Notes and references

- (a) N. Savage, *Nat. Photonics*, 2007, **1**, 83; (b) K. M. Ok, E. O. Chi and P. S. Halasyamani, *Chem. Soc. Rev.*, 2006, **35**, 710; (c) H. Lee and K. M. Ok, *Bull. Korean Chem. Soc.*, 2020, **41**, 139.
- (a) B. F. Levine, *Phys. Rev. Lett.*, 1970, **25**, 440; (b) C. Chen, T. Sasaki, R. Li, Y. Wu, Z. Lin, Y. Mori, Z. Hu, J. Wang, S. Uda, M. Yoshimura and Y. Kaneda, *Nonlinear Optical Borate Crystals, Principles and Applications*, Wiley-VCH, Weinheim, Germany, 2012, pp. 15–116; (c) J. Jeon, J. Lee and T.-S. You, *Bull. Korean Chem. Soc.*, 2018, **39**, 1066.
- (a) C. Chen, *Sci. Sin.*, 1979, **22**, 756; (b) C. Chen and G. Liu, *Annu. Rev. Mater. Sci.*, 1986, **16**, 203; (c) C. T. Chen, Y. C. Wu and R. K. Li, *Int. Rev. Phys. Chem.*, 1989, **8**, 65.
- 4 C. T. Chen, B. C. Wu, A. D. Jiang and G. M. You, *Sci. Sin. Ser. B*, 1985, **28**, 23.
- 5 C. T. Chen, Y. C. Wu, A. D. Jiang, B. C. Wu, G. M. You, R. K. Li and S. J. Lin, *J. Opt. Soc. Am. B*, 1989, **6**, 616.
- 6 L. Mei, Y. Wang, C. Chen and B. Wu, *J. Appl. Phys.*, 1993, **74**, 7014.
- 7 C. T. Chen, Y. B. Wang, B. C. Wu, K. C. Wu, W. L. Zeng and L. H. Yu, *Nature*, 1995, **373**, 322.
- 8 (a) Y. T. Zhang, Y. Long, X. H. Dong, L. Wang, L. Huang, H. M. Zeng, Z. E. Lin, X. Wang and G. H. Zou, *Chem. Commun.*, 2019, **55**, 4538; (b) Q. F. Li, G. H. Zou, C. S. Lin and N. Ye, *New J. Chem.*, 2016, **40**, 2243; (c) Q. Wang, F. F. He, L. Huang, D. J. Gao, J. Bi and G. H. Zou, *Cryst. Growth Des.*, 2018, **18**, 3644.
- 9 (a) Y. X. Song, M. Luo, C. S. Lin and N. Ye, *Chem. Mater.*, 2017, **29**, 896; (b) L. Wang, F. Yang, X. Y. Zhao, L. Huang, D. J. Gao, J. Bi, X. Wang and G. H. Zou, *Dalton Trans.*, 2019, **48**, 15144; (c) X. H. Dong, L. Huang, Q. Y. Liu, H. M. Zeng, Z. E. Lin, D. J. G. Xu and G. H. Zou, *Chem. Commun.*, 2018, **54**, 5792.
- 10 (a) S. G. Zhao, X. Y. Yang, Y. Yang, X. J. Kuang, F. Q. Lu, P. Shan, Z. H. Sun, Z. S. Lin, M. C. Hong and J. H. Luo, *J. Am. Chem. Soc.*, 2018, **140**, 1592; (b) J. Chen, L. Xiong, L. Chen and L. M. Wu, *J. Am. Chem. Soc.*, 2018, **140**, 14082.
- 11 (a) F. F. He, L. Wang, C. F. Hu, J. Zhou, Q. Li, L. Huang, D. J. Gao, J. Bi, X. Wang and G. H. Zou, *Dalton Trans.*, 2018, **47**, 17486; (b) Q. Wang, L. Wang, X. Y. Zhao, L. Huang, D. J. Gao, J. Bi, X. Wang and G. H. Zou, *Inorg. Chem. Front.*, 2019, **6**, 3125; (c) F. F. He, Y. L. Deng, X. Y. Zhao, L. Huang, D. J. Gao, J. Bi, X. Wang and G. H. Zou, *J. Mater. Chem. C*, 2019, **7**, 5748.
- 12 K. M. Ok, *Acc. Chem. Res.*, 2016, **49**, 2774.
- 13 (a) J. Y. Guo, A. Tudi, S. J. Han, Z. H. Yang and S. L. Pan, *Angew. Chem., Int. Ed.*, 2019, **58**, 17675; (b) F. F. Mao, C. L. Hu, X. Xu, D. Yan, B. P. Yang and J. G. Mao, *Angew. Chem., Int. Ed.*, 2017, **56**, 2151.



14 Z. G. Xia and K. R. Poeppelmeier, *Acc. Chem. Res.*, 2017, **50**, 1222.

15 (a) G. H. Zou, H. Jo, S. Lim, T. You and K. M. Ok, *Angew. Chem., Int. Ed.*, 2018, **57**, 8619; (b) G. H. Zou, Z. Lin, H. M. Zeng, H. Jo, S. Lim, T. You and K. M. Ok, *Chem. Sci.*, 2018, **9**, 8957.

16 Y. Song, M. Luo, F. Liang, N. Ye and Z. Lin, *Chem. Commun.*, 2018, **54**, 1445.

17 (a) T. T. Tran, J. Young, J. M. Rondinelli and P. S. Halasyamani, *J. Am. Chem. Soc.*, 2017, **139**, 1285; (b) G. H. Zou, N. Ye, L. Huang and X. S. Lin, *J. Am. Chem. Soc.*, 2011, **133**, 20001; (c) G. Yang, G. Peng, N. Ye, J. Wang, M. Luo, T. Yan and Y. Zhou, *Chem. Mater.*, 2015, **27**, 7520.

18 (a) G. H. Zou, Z. J. Ma, K. C. Wu and N. Ye, *J. Mater. Chem.*, 2012, **22**, 19911; (b) G. H. Zou, L. Huang, H. Q. Cai, S. C. Wang and N. Ye, *New J. Chem.*, 2014, **38**, 6186.

19 G. Zou, C. Lin, H. Jo, G. Nam, T. S. You and K. M. Ok, *Angew. Chem., Int. Ed.*, 2016, **55**, 12078.

20 (a) M. Luo, Y. Song, F. Liang, N. Ye and Z. Lin, *Inorg. Chem. Front.*, 2018, **5**, 916; (b) H. Yu, N. Koocher, J. Rondinelli and P. S. Halasyamani, *Angew. Chem., Int. Ed.*, 2018, **57**, 6100.

21 H. Huang, J. Yao, Z. Lin, X. Wang, R. He, W. Yao, N. Zhai and C. Chen, *Chem. Mater.*, 2011, **23**, 5457.

22 Z. G. Hu, T. Higashiyama, M. Yoshimura, Y. K. Yap, Y. Mori and T. Sasaki, *Jpn. J. Appl. Phys.*, 1998, **37**, 1093.

23 Z. G. Hu, M. Yoshimura, K. Muramatsu, Y. Mori and T. Sasaki, *Jpn. J. Appl. Phys.*, 2002, **41**, L1131.

24 N. Ye, W. R. Zeng, B. C. Wu, X. Y. Huang and C. T. Chen, *Z. Kristallogr.*, 1998, **213**, 452.

25 Z. H. Yang, B. H. Lei, W. Y. Zhang and S. L. Pan, *Chem. Mater.*, 2019, **31**, 2807.

26 X. L. Cao, C. L. Hu, X. Xu, F. Kong and J. G. Mao, *Chem. Commun.*, 2013, **49**, 9965.

27 M. Liang, C. Hu, F. Kong and J. Mao, *J. Am. Chem. Soc.*, 2016, **138**, 9433.

28 S. D. Nguyen, J. Yeon, S. H. Kim and P. S. Halasyamani, *J. Am. Chem. Soc.*, 2011, **133**, 12422.

29 J. M. Hughes and J. Rakovan, *Rev. Mineral. Geochem.*, 2002, **45**, 1.

30 (a) Y. Fei, B. H. Chai, C. A. Ebbers, Z. M. Liao, K. I. Schaffers and P. Thelin, *J. Cryst. Growth*, 2006, **290**, 301; (b) H. J. Zhang, H. D. Jiang, J. Y. Wang, X. B. Hu, G. W. Yu, W. T. Yu and M. H. Jiang, *Appl. Phys. A*, 2004, **78**, 889; (c) G. Aka, A. Kahn-Harari, F. Mougel, D. Vivien, F. Salin, P. Coquelin and J. P. Damelet, *J. Opt. Soc. Am. B*, 1997, **14**, 2238.

31 W. L. Zhang, W.-D. Cheng, H. Zhang, L. Geng, C.-S. Lin and Z.-Z. He, *J. Am. Chem. Soc.*, 2010, **132**, 1508.

32 M. Luo, G. H. Zou, N. Ye, C. S. Lin and W. D. Cheng, *Chem. Mater.*, 2013, **25**, 3147.

33 M. Luo, Y. Song, C. Lin, N. Ye, W. Cheng and X. Long, *Chem. Mater.*, 2016, **28**, 2301.

34 J. D. Bierlein and H. Vanherzele, *J. Opt. Soc. Am. B*, 1989, **6**, 622.

35 (a) F. F. He, Q. Wang, C. F. Hu, W. He, X. Y. Luo, L. Huang, D. J. Gao, J. Bi, X. Wang and G. H. Zou, *Cryst. Growth Des.*, 2018, **18**, 6239; (b) X. H. Dong, L. Huang, C. F. Hu, H. M. Zeng, Z. E. Lin, X. Wang, K. M. Ok and G. H. Zou, *Angew. Chem., Int. Ed.*, 2019, **58**, 6528.

36 F. Yang, L. J. Huang, X. Y. Zhao, L. Huang, D. J. Gao, J. Bi, X. Wang and G. H. Zou, *J. Mater. Chem. C*, 2019, **7**, 8131.

37 K. Chen, Y. Yang, G. Peng, S. Yang, T. Yan, H. Fan, Z. Lin and N. Ye, *J. Mater. Chem. C*, 2019, **7**, 9900.

38 J. Chen, C.-L. Hu, F.-F. Mao, J.-H. Feng and J.-G. Mao, *Angew. Chem., Int. Ed.*, 2019, **58**, 2098.

